J. prakt. Chem. 338 (1996) 620–626

Journal für praktische Chemie
Chemiker-Zeitung

Dissolution Kinetics of Single Fluoroapatite Crystals in Phosphoric Acid Solution under the Conditions of the Wet-Process Phosphoric Acid Production

Sergey V. Dorozhkin

Moscow (Russia), Research Institute of Fertilizers and Insectofungicides

Received February 15th, 1995 respectively September 12th, 1995

Abstract. The dissolution process for natural single fluoroapatite (FAP) crystals is studied in phosphoric acid solutions, containing the main inorganic impurities present in the industrial wet-process phosphoric acid production. A special flow device providing constant dissolution conditions was used for this purpose. The device gave the possibility to obtain new information about the dynamics concerning shape and size of each individual FAP crystal during its dissolution. Dissolution rates for the FAP crystals were measured under various conditions. The process of epitaxial coating of the FAP crystal surface by $CaSO_4 \cdot 0.5 H_2O$ was also studied. Without coating formation the single FAP crystals always dissolved with continuously increasing rates for all crystal faces. The measured values of dissolution rates are applied to computer simulation of industrial reactors.

Phosphorus is one of the main chemical elements which is absolutely necessary in agriculture for producing large crops. Books dedicated to phosphorus and its fertilizer production [1–5] inform, that most of all phosphorus-containing inorganic fertilizers are produced from one intermediate product – wet-process phosphoric acid. The authors of [1–5] also inform that the typical way for industrial wet-process phosphoric acid production includes dissolution of any natural phosphate mineral in a mixture of phosphoric and sulfuric acids with subsequent separation of calcium sulfate (by-product) from the phosphoric acid solution.

The present paper deals with the dissolution process of individual crystals of natural phosphate mineral. There are many scientific investigations in the field of kinetics and mechanism of phosphate ore dissolution in phosphoric acid solutions under conditions, close to the industrial ones. Some of them are mentioned in references [1–13] and references therein. The earlier level of knowledge became the theoretical basis for designing and construction of all modern phosphoric acid production plants. However, the papers mentioned were only devoted to the dissolution process of great numbers of natural crystals (about 10^4 crystals and more). As a result there is no information about the dissolution laws for each individual crystal in acid solution. But such information is very important for better understanding and adequate simulation of the processes in an industrial reactor.

Experimental

Single crystals of natural Khibin (Kola) fluoroapatite (FAP) were used as the phosphate source in all experiments. This choice has been made for the following reasons: 1. Khibin (Kola) FAP is a magmatic kind of natural phosphate rocks, having good crystallised single crystals; 2. Its chemical composition is very close to $Ca_{10}(PO_4)_6F_2$; 3. The FAP crystals are easily to distinguish and to separate from crystals of other admixed minerals under an optical microscope by using a needle; 4. Khibin (Kola) rock is the most popular kind of natural phosphate rock for the fertilizer industry in the former USSR.

A special flow apparatus was constructed for the experimental investigations (Fig. 1). One or several FAP crystals (4) were placed on a special thermostatic holder (6), having a shape of the shallow spoon. Then the holder with FAP crystals was placed in a stream of phosphoric acid. Using a large quantity (about 1 kg) of acid solution in the thermostatic flask (1) and a small weight (about 1 mg) of dissolving FAP crystals (4), the composition of the flowing solution remains constant during the time of the experiment. Any changes of the crystal shape and size during their dissolution were observed and filmed by means of an optical polarization microscope MIN-8 type (5), provided with a photographic adapter MFNE-

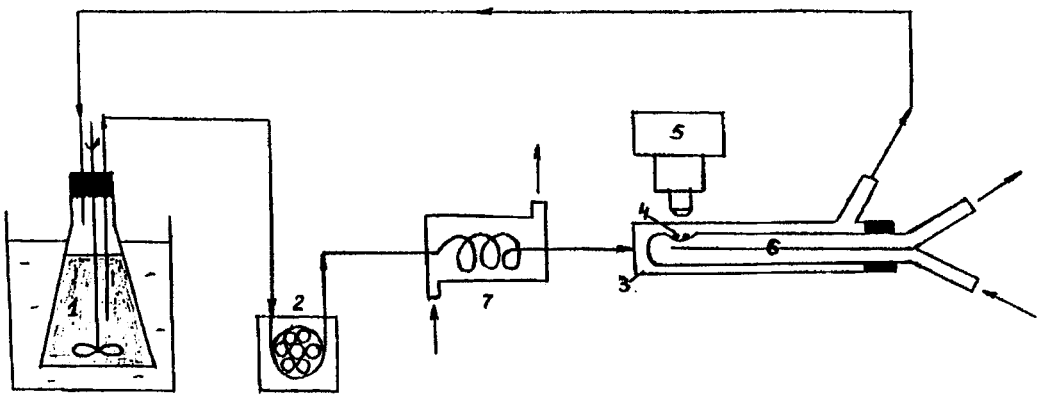

Fig. 1 Experimental flow device: 1 – thermostatic flask with acid solution, 2 – peristaltic pump, 3 – dish made from optical quartz, 4 – FAP crystals, 5 – polarization microscope with photographic adapter, 6 – thermostatic holder, 7 – heater

1U4.2 type (both made by LOMO, Russia). The main merit of this installation is the possibility to observe and film the dissolution process for each individual FAP crystal. But it is restricted by the microscope magnification (up to 100 times) and the stream rates of the acid (not more than $Re > 100$ hydrodynamics). When $Re > 100$, the non-fixed FAP crystals are usually washed away from the holder (especially in the final phases of their dissolution). Attempts to glue the FAP crystals to the holder always resulted in surface pollution by glue components. For some investigations a scanning electron microscope JSM-35CF was also used.

The experimental concentrations were as follows: phosphoric acid: 0 – 16 mol/dm^3, sulfuric acid in 7.2 M H_3PO_4 solution: 0–0.4 mol/dm^3, calcium sulfate in 7.2 M H_3PO_4 solution: 0–0.08 mol/dm^3, calcium monophosphate in 7.2 M H_3PO_4 solution: 0–1.1 mol/dm^3, H_2SiF_6 in 7.2 M H_3PO_4 solution 0–0.7 mol/dm^3. Initial crystal size (R_{eq}): 25–1000 μm. Temperature: 60–90 °C, *Re* hydrodynamics < 100. All reagents were "pure grade" quality made by the Russian company REACHIM.

Results

The flow device experiments resulted in a series of successive photographs for each individual dissolving FAP crystal or group of crystals (Figs. 2 and 3). The comparison of these photographs with each other has made possible for the first time to show the change of their size and shape during the dissolution. To aid calculation of dissolution rates the successive photographs were printed on one sheet of photo-paper (Fig. 4). Here the distances between adjacent contours divided by the time interval correspond to the rate values of the FAP crystal dissolution in the selected direction for the selected time interval $-G_{local}$ (μm/s). The averaged G_{local} values for all directions during the selected time interval is an average linear dissolution rate during this time interval $-G_{time}$ (μm/s) and all averaged G_{time} values give an average linear dissolution rate for the investigated crystal $-G_{cr}$ (μm/s). The last value is easy to recalculate to the value of an average mass dissolution rate from the surface unit $-G_{mass}$ (kg/m^{2}s):

$$G_{mass} = 10^6 \cdot \rho_{FAP} \cdot G_{cr}. \quad (1)$$

Here: 10^6 – correction factor from μm to m, $\rho_{FAP} = 3200$ kg/m^3 – FAP density.

For G_{cr} values calculation the G_{local} values from 12 different directions for each FAP crystal were averaged according to Fig. 4. Having been passed through industrial mills during their extraction from natural deposit, the FAP crystals always had an accidental irregular shape. So the largest crystal size ($\varphi = 0$ in Fig. 4) was chosen as the initial one. The other 11 directions differ for 30° each. These 12 directions are sufficient enough for the calculation of G_{cr} values, and it was shown that by using, for example, 24 directions, the exactness of G_{cr} values increases only by ± 1 %.

We found that the FAP crystals dissolve only from their surface without any disintegration (Figs. 2, 3). But different small parts of the FAP crystal surface (about 1–5 μm) dissolve with different local rates with parameters close to a Gauss distribution which has only one maximum. So the dissolution process can be described only by values of the average dissolution rate and its fluctuation coefficient [14]. Crystal cleavage was extremely rare during dissolution and occurred only when the initial crystals contained cracks. We applied the values of the face dissolution linear rates as the main characteristics of the dissolution rate instead of the well-known conversion coefficient values [1–13, 15, 16]. The advantage of the face linear dissolution rates compared with the conversion coefficient is obvious. Knowing the first values it is easy to calculate crystal sizes for any

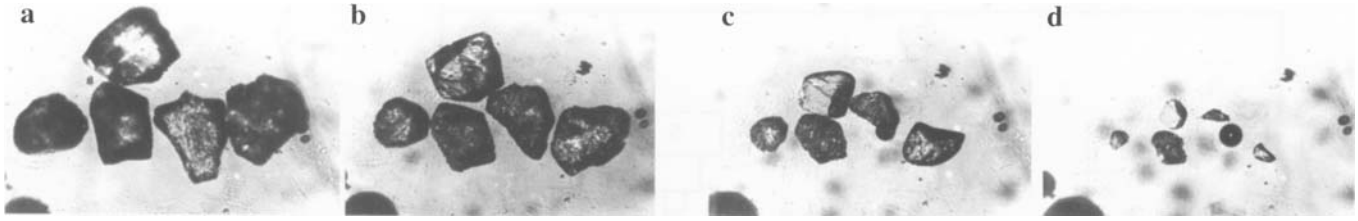

Fig. 2 Example of the dissolution of individual FAP crystals under conditions preventing any coating formation. Experimental conditions: 52% H_3PO_4, t = 80 °C, $Re \leq 100$, 75 μm ≤ R_{eq} ≤ 125 μm. Dissolution time: a – 20 s, b – 5 min, c – 10 min, d – 14.5 min. Magnification × 90. Horizontal field width = 1 mm.

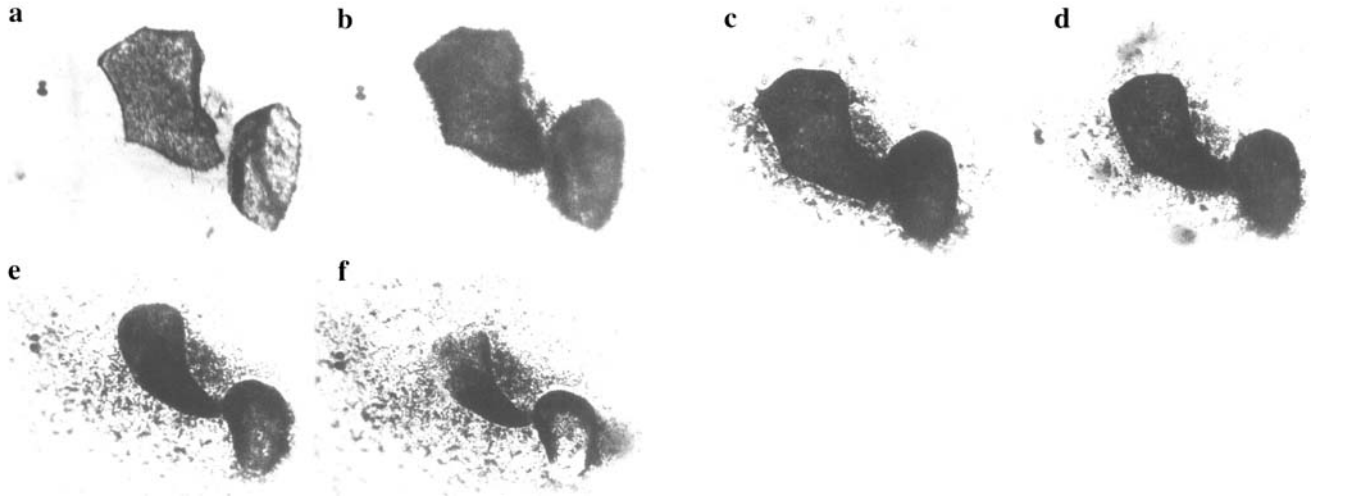

Fig. 3 Example of the dissolution of individual FAP crystals under conditions of $CaSO_4 \cdot 0.5H_2O$ coating formation. Experimental conditions: 52% H_3PO_4, 2% H_2SO_4, t = 80 °C, $Re \leq 100$, 75 μm ≤ R_{eq} ≤ 125 μm. Dissolution time: a – 15 s, b – 1 min, c – 45 min, d – 90 min, e – 128.5 min, f – 135 min. Magnification × 90. Horizontal field width = 1 mm

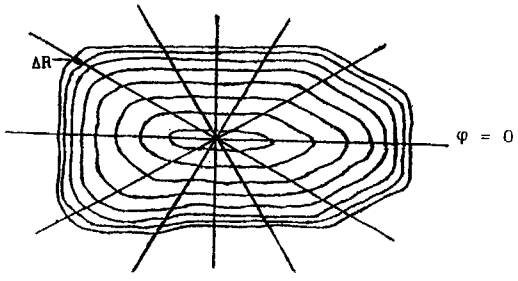

Fig. 4 Dissolution of a FAP crystal

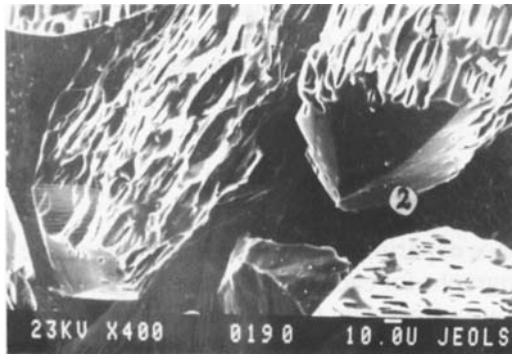

Fig. 5 Example of etching mechanism difference between prismatic (1) and pyramidal (2) faces for the FAP crystals. Experimental conditions: 52% H_3PO_4, t = 80 °C, $Re \leq 3000$, 75 μm ≤ R_{eq} ≤ 125 μm. The bar amounts to 10 μm

FAP crystal or group of crystals at any time of their dissolution, which is very difficult by using the traditional conversion coefficient values.

Sometimes it is possible to find regular FAP crystals among natural rocks. Their comparison with the habit of an ideal FAP crystal [17] resulted in the determination of the dissolution rates for main FAP crystal faces. We found that dissolution rates for prismatic and pinacoid faces are similar and about 1.5 lower than those for pyramidal ones. This phenomenon has been explained by means of scanning electron microscopy. We found different etching processes for different crystallographic faces [18]. Unlike pyramidal faces prismatic and pinacoid ones were always covered by etch pits (Fig. 5) which were sites of fastest dissolution rates [17]. We found that in our case pyramidal faces were similar to

etch pit's crystallographic faces, i. e. from the crystallographic point of view each pyramidal face was something like a big pit, but upside down.

Moreover, the crystals of natural FAP always dissolve in acids with continuously increasing rates for all faces (Fig. 4). This is indicated by the increase of the distances ΔR between adjacent contours during equal time intervals. The change of the relative size of FAP crystals (R/R_o) *versus* relative time (τ/τ_o) is shown in Fig. 6 (curve 1). To the end of the dissolution process, the G_{time} value were found to increase to 1.6 times [14].

We found that under the chosen experimental conditions the dissolution rates for FAP crystal surface depend neither on the velocity of the acid's flow around the crystals nor the initial crystal size. Regardless of the dissolution conditions, where epitaxial coatings of any by-products were not formed, the effect of dissolution acceleration according to Fig. 6 (curve 1) was always observed. Consequently, the acceleration effect is found to be a property of the FAP crystals themselves and depends only on their dislocation structure [14].

However, it may be difficult to take into account the acceleration effect for the simulation of real technical

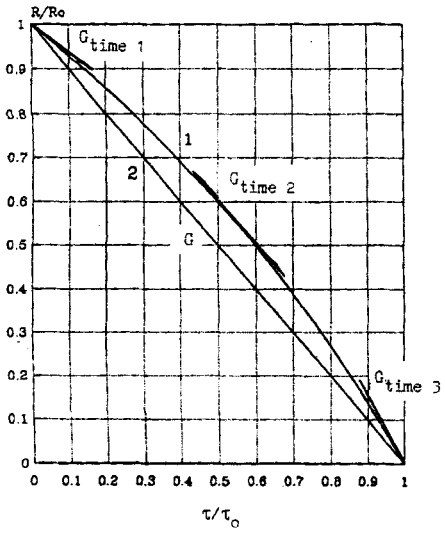

Fig. 6 Comparison of the average dissolution rates G_{cr} (curve 1) and G (line 2).

$$G_{cr} = \frac{1}{n}\sum_{i=1}^{n} G_{time,i} \qquad G_{time,3} = 1.6 G_{time,1}$$

reactors. So, for the simplicity of the process simulation we propose the other average value of the linear dissolution rate G (μm/s):

$$G = \frac{1}{n}\cdot\sum_{i=1}^{n} G_i = \frac{1}{n}\cdot\sum_{i=1}^{n}\left(\frac{R_i, eq}{\tau_{i,o}}\right) \qquad (2)$$

G_i – dissolution rate averaged to all directions for i-crystal, μm/s; n – number of FAP crystals; $R_{i,eq}$ – equivalent radius for i-crystal, μm; $\tau_{i,o}$ – full dissolution time for i-crystal, s.

The comparison of the average dissolution rates G_{cr} and G_i for one FAP crystal is shown in Fig. 6. Here G_{cr} – is an averaged value from all tangents to curve 1 (each tangent is equal to the G_{time} value), and G_i is the straight line 2. Fig. 6 also shows, that the correlation between G_i and G_{cr} values changes during the dissolution process. When $0 \le \tau_i/\tau_{i,o} < 0.5$ $G_i > G_{cr}$; when $\tau_i/\tau_{i,o} = 0.5$ $G_i = G_{cr}$ and when $0.5 < \tau_i/\tau_{i,o} \le 1.0$ $G_i < G_{cr}$ (τ_i is the current dissolution time). According to the demands of the fertilizer industry experimental plots of the G values, averaged from G_i values for n = 30–50 FAP crystals, as a function of dissolution parameters were measured (Figs. 7–10).

Discussion

The relations in Fig. 7–10 show, that G has a maximum in pure phosphoric acid and depends highly on the amount of impurities. Beside strong mineral acids such as HNO_3 and HCl [9] all other usual technological impurities decrease the G values. The obtained negative influence of calcium in the phosphoric acid solution on the G values (Fig. 7) has been explained earlier in the literature by neutralization of a first H^+ ion [1–5].

The G value dependence on the amount of H_2SO_4 in the phosphoric acid solution (Fig. 8) corresponds to similar results obtained in a laboratory reactor with agitator [19]. But, unlike to the results of [19], in which only the final dissolution stages were accurately measured

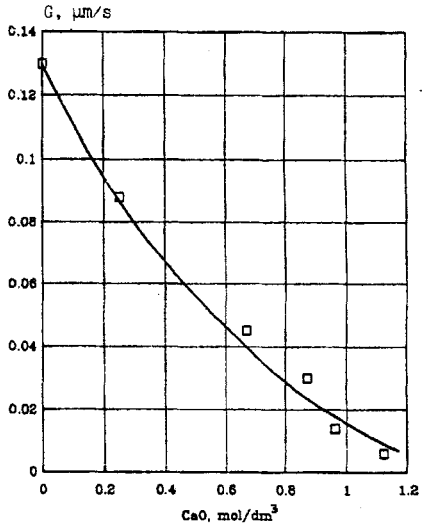

Fig. 7 Dependence of the FAP dissolution rate on the amount of CaO in phosphoric acid solution. Experimental conditions: 52% H_3PO_4, t = 80 °C, $Re \le$ 100, 75 μm $\le R_{eq} \le$ 125 μm

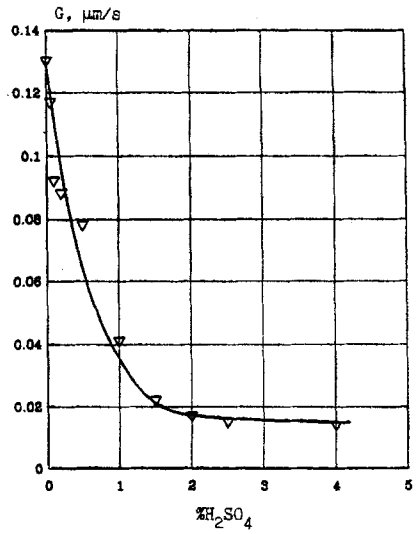

Fig. 8 Dependence of FAP dissolution rate on the amount of H_2SO_4 in phosphoric acid solution. Experimental conditions: 52% H_3PO_4, t = 80 °C, $Re \leq 100$, 75 μm ≤ R_{eq} ≤ 125 μm

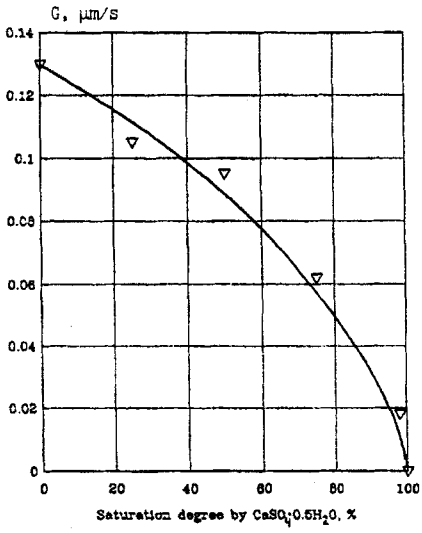

Fig. 10 Dependence of FAP dissolution rate on the amount of $CaSO_4 \cdot 0.5\ H_2O$ in phosphoric acid solution. Experimental conditions: 52% H_3PO_4, t = 80 °C, $Re \leq 100$, 75 μm ≤ R_{eq} ≤ 125 μm

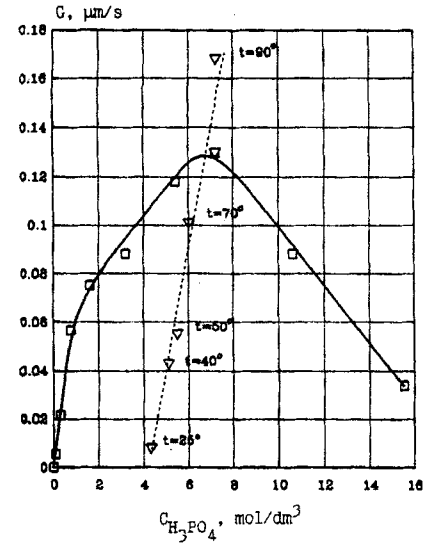

Fig. 9 Dependence of FAP dissolution rate on the concentration of H_3PO_4 in solution. Experimental conditions: t = 80 °C, $Re \leq 100$, 75 μm ≤ R_{eq} ≤ 125 μm

(because during the initial period of dissolution it was difficult to distinguish the experimental curves from each other), the flow device used in the present work has made possible to determine the negative influence of H_2SO_4 from the very beginning.

The very important problem of epitaxial $CaSO_4 \cdot 0.5\ H_2O$ coating formation on the FAP crystal surface [2–5] was also studied by means of our laboratory device (Fig. 3). It is interesting to note, that under laminar hydrodynamics the FAP crystals were quickly covered by $CaSO_4 \cdot 0.5\ H_2O$ coatings (during 1–2 minutes, when there were more than 1.5% H_2SO_4 in phosphoric acid solution). A growing of long needle-like $CaSO_4 \cdot 0.5\ H_2O$ crystals on the FAP surface at the beginning of dissolution could easily be seen (Fig. 3a, b). Then, the dissolution process for the covered by $CaSO_4 \cdot 0.5\ H_2O$ FAP particles continued very slowly without changes of common external geometric size of FAP and coating (Fig. 3c, d). During the last dissolution period the coating became transparent and disappeared during 5–7 minutes (Fig. 3e, f) [20]. So, there were some specific conditions for a stable quasi-equilibrium between the growing of $CaSO_4 \cdot 0.5\ H_2O$ crystals inside and its dissolution outside. This quasi-equilibrium is stable only till the last moments of existing FAP crystals under the $CaSO_4 \cdot 0.5\ H_2O$ coating.

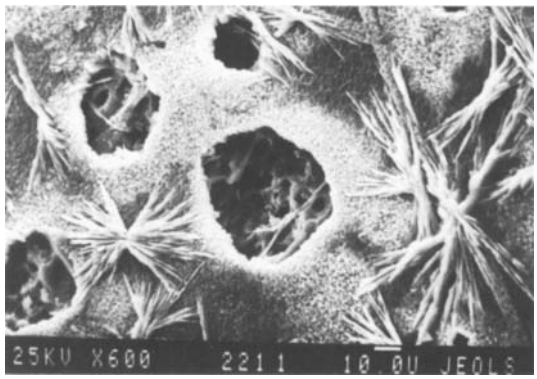

Fig. 11 Example of the FAP crystal with knocked out fragments of $CaSO_4 \cdot 0.5\ H_2O$ coatings. Experimental conditions: 52% H_3PO_4, 2% H_2SO_4, t = 80 °C, $Re \approx 5\,000$, 75 μm ≤ R_{eq} ≤ 125 μm. The bar amounts to 10 μm

The dissolution times and rates of Figs. 2 and 3 differ by 10 times. An other words, an increase of the H_2SO_4 concentration in phosphoric acid solution from 0 to 2% decreases the dissolution rate by 10 times. The dissolution acceleration (Figs. 4, 6) increases the dissolution rate not more than 1.6 times [14]. So, under conditions of epitaxial coating formation the acceleration effect needs not to be taken into consideration at all.

The G dependence on the concentration of H_3PO_4 in solution at t = 80 °C is shown in Fig. 9, which fully corresponds to results found earlier at 25, 40, 50, 70 and 90 °C [1, 6, 21]. The points of maximal dissolution rates of FAP crystals at these temperatures are plotted in Fig. 9. The results show, that the point of the maximal dissolution rate moves to higher concentrations of the phosphoric acid solution when the temperature increases. It was explained earlier by differences of the $CaHPO_4$ and $Ca(H_2PO_4)_2$ solubilities at different temperatures [1, 6, 21].

The G value dependence on temperature, unlike the earlier published results for pure H_3PO_4 solutions [1], was determined for phosphoric acid solutions, containing 3.5% CaO (or 0.86 mol/dm^3 $Ca(H_2PO_4)_2$). In pure H_3PO_4 solutions in the concentration range of 10–60% H_3PO_4 the dissolution rate coefficient for FAP was found rising 1.30–1.40-fold for each 10 °C [1]. Having recalculated this value to an average dissolution activation energy value we found: $E_{act} \approx 25 \pm 2$ kJ/mol. Our investigations have shown that a presence of 3.5% CaO in 7.2 M (or 52%) H_3PO_4 solution increases the dissolution activation energy twice: $E_{act} \approx 48 \pm 2$ kJ/mol. The strong dependence of E_{act} on the calcium content in solution also explains the negative influence of CaO to the G value (Fig. 7).

But the G value dependence on the amount of $CaSO_4 \cdot 0.5 H_2O$ in the phosphoric acid solution is more interesting (Fig. 10). Our results show, that phosphoric acid solutions previously saturated with $CaSO_4 \cdot 0.5 H_2O$ dissolve FAP crystals infinitely slowly in spite of the low total Ca^{2+} and SO_4^{2-} concentrations (only about 0.5% for each ion). Figs. 7 and 8 show, that these ions in such low concentrations in phosphoric acid separately do not decrease the dissolution rate so much. This phenomenon is explained by the formation of epitaxial $CaSO_4 \cdot 0.5 H_2O$ coatings on the FAP crystal surface. The coatings fully block the initial FAP crystal surface and prevent its dissolution. Unlike coating in the mixture of pure H_3PO_4 and H_2SO_4 acids (Figs. 3, 8), additional calcium cations in the solution prevent the dissolution $CaSO_4 \cdot 0.5H_2O$ crystals from outside completely. As the result the dissolution rate for FAP is zero in phosphoric acid solutions saturated by calcium sulfate.

However, it is well-known [1–5], that in industry phosphate rock is always dissolved in phosphoric acid solutions saturated or even supersaturated with $CaSO_4 \cdot x H_2O$ (where x = 0, 0.5, 2). The discrepancy between the laboratory and the industrial conditions is easily explained by differences in hydrodynamics. There are always high agitation regimes in industrial dissolving reactors, so the energy of colliding particles is high enough for knocking out fragments of epitaxial $CaSO_4 \cdot 0.5 H_2O$ coatings. At such sites the etched FAP surface becomes uncovered (Fig. 11) which increases the dissolution. Nevertheless in stagnated zones of chemical reactors there may be hydrodynamics conditions, preventing the dissolution process. In the former USSR, workers sometimes found such non-dissolved phosphate particles in phosphogypsum deposits during the updating and reconstruction of industrial wet-process reactors. The results point to the importance of good agitation in industrial reactors.

We also found that the G value dependence on the amount of H_2SiF_6 in phosphoric acid is small. Our results point to the independence of the G values on increasing H_2SiF_6 concentrations from 1 to 6% H_2SiF_6 in phosphoric acid solution. Possibly, this phenomenon may be explained by similar values of the first dissociation constants for H_3PO_4 and H_2SiF_6.

By means of the obtained data it becomes possible to simulate the dissolution process only knowing the initial size distribution of the phosphate rock particles and the initial chemical composition of acid solution. An example of simulation and construction of an original dissolution reactor for the wet-process phosphoric acid production basing on the obtained results has been published earlier [22].

The obtained experimental results about the process of the single FAP crystals dissolution (Figs. 2–11) show, that new intensification principles of phosphate rock dissolution require a separation of phosphate rock dissolution and calcium sulfate crystallization stages. The same conclusion was also established by some other investigators: (i) after studying of $CaSO_4 \cdot 0.5 H_2O$ crystallization mechanism [23–25], (ii) after creation a technology of phosphoric acid production without cadmium content [12, 13], (iii) US. patent No. 4,828,811 [26].

Notation

E_{act}	activation energy
G	average value of all linear dissolution rates in equation 2
G_{local}	local value of linear dissolution rate in a selected direction and the selected time interval
G_{time}	average value of local linear dissolution rates for all directions and the selected time interval
G_{cr}	average value of all linear dissolution rates for all directions and all time intervals
G_{mass}	average mass dissolution rate
n	number of the FAP crystals

ΔR local distance between next adjacent contours
R current size of a FAP crystal
R_o initial size of a FAP crystal
R_{eq} equivalent radius of a FAP crystal
ρ_{FAP} FAP density
φ initial crystal direction in Fig. 4
τ current dissolution time for a FAP crystal
τ_o full dissolution time for a FAP crystal

References

[1] M. L. Chepelevetskii, E. B. Brutskus, Superphosphate (physico-chemical foundations of its manufacturing). Moscow. State Chemistry Publisher, 1958, p. 272

[2] A. V. Slack, Ed., Phosphoric Acid. Fertilizer Science and Technology Series. Marcel Dekker, New York 1967, vol. 1– 2, p. 1159

[3] R. Noyes, Phosphoric Acid by the Wet Process. Noyes Development Corporation, London 1967, p. 282

[4] B. A. Kopylev, Wet process phosphoric acid technology, 2nd Ed. Leningrad, Chemistry Publisher 1981, p. 221

[5] P. Becker, Phosphates and Phosphoric Acid. 2nd Ed. Fertilizer Science and Technology Series. Marcel Dekker, New York 1989, p. 740

[6] M. L. Chepelevetskii, Physico-chemical basis of phosphate processing by acids. D. Sc. (Chemistry) thesis: USSR, Moscow Research Institute of Fertilizers 1946, p. 370

[7] E. V. Juzhnaja, Decomposition kinetics of apatite and calcite by acids. Ph. D. (Chemistry) thesis. USSR, Moscow, Research Institute of Fertilizers 1956, p. 142

[8] S. M. Janikowski, N. Robinson, W. F. Sheldric, Insoluble phosphate losses in phosphoric acid manufacture by the wet process: theory and experimental techniques. Presented at the 18th Meeting of Fertilizer Society. London 1964, p. 3

[9] I. I. Orekhov, Investigations in a field of natural phosphate processing to fertilizers by acids. D. Sc. (Engineering) thesis. USSR, Leningrad, Technological Institute 1972, p. 350

[10] V. V. Kochetkova, Wet-process phosphoric acid technological improvement on the base of peculiarity of apatite dissolution. Ph. D. (Engineering) thesis. USSR, Moscow Research Institute of Fertilizers 1984, p. 155

[11] J. L. Kim, Demineralization of calcium phosphates and other minerals. Ph. D. thesis. USA, University of Minnesota 1985, p. 187

[12] S. Van der Sluis, A clean technology phosphoric acid process. Ph. D. thesis. The Netherlands, Delft University 1987, p. 202

[13] S. Van der Sluis, Y. Meszaros, W. G. J. Marchee, H. A. Wesselingh, G. M. Van Rosmalen, Ind. Eng. Chem. Res. **26** (1987) 2501

[14] I. V. Melikhov, S. V. Dorozhkin, A. L. Nikolaev, E. D. Kozlovskaya, V. N. Rudin, Russian J. Phys. Chem. **64** (1990) 3242

[15] C. E. Calmanovici, M. Giulietti, Ind. Eng. Chem. Res. **29** (1990) 482

[16] S. S. Elnashaie, T. F. Al-Fariss, S. M. A. Razik, H. A. Ibrahim, Ind. Eng. Chem. Res. **29** (1990) 2389

[17] K. Frye, Ed., The Encyclopedia of Mineralogy. Encyclopedia of earth science, volume IV, B. Hutchinson Ross Publishing Company 1981, p. 794

[18] S. V. Dorozhkin, V. N. Rudin, Russian J. Chemical Industry **2** (1992) 96

[19] A. V. Grinevich, V. V. Kochetkova, P. V. Klassen, A. V. Alexandrov, Russian J. Appl. Chem. **56** (1983) 1359

[20] I. V. Melikhov, S. V. Dorozhkin, A. L. Nikolaev, V. N. Rudin, Bull. Acad. Sci. Russia (Inorganic Materials series) **28** (1992) 872

[21] M. L. Chepelevetskii, E. B. Brutskus, K. S. Krasnov, E. V. Juzhnaja, Russian J. Inorg. Chem. **1** (1956) 1512

[22] B. M. Dolgonosov, S. V. Dorozhkin, I. V. Melikhov, V. N. Rudin, Russian J. Theor. Foundat. Chem. Technol. **28** (1994) 359

[23] I. V. Melikhov, I. E. Mikheeva, V. N. Rudin, Russian J. Crystallography **34** (1989) 1272

[24] I. V. Melikhov, I. E. Mikheeva, V. N. Rudin, Russian J. Theor. Foundat. Chem. Technol. **19** (1985) 742

[25] I. V. Melikhov, I. E. Mikheeva, V. N. Rudin, Russian Colloid J. **50** (1988) 885

[26] G. M. Derdall, W. R. Ericson, R. L. Phinney, J. D. Wilson, U. S. patent No. 4,828,811. Potash corp. No. 76608. Published 09th May (1989)

Address for correspondence:
Dr. S. V. Dorozhkin
Kudrinskaja sq. 1 - 155
123242 Moscow D-242
Russia